



This is a repository copy of *Extraction of uranium from non-saline and hypersaline conditions using iminodiacetic acid chelating resin Purolite S930+*.

White Rose Research Online URL for this paper:  
<http://eprints.whiterose.ac.uk/129525/>

Version: Accepted Version

---

**Article:**

Amphlett, J.T.M., Sharrad, C.A. and Ogden, M.D. [orcid.org/0000-0002-1056-5799](https://orcid.org/0000-0002-1056-5799) (2018) Extraction of uranium from non-saline and hypersaline conditions using iminodiacetic acid chelating resin Purolite S930+. *Chemical Engineering Journal*, 342. pp. 133-141. ISSN 1385-8947

<https://doi.org/10.1016/j.cej.2018.01.090>

---

**Reuse**

This article is distributed under the terms of the Creative Commons Attribution-NonCommercial-NoDerivs (CC BY-NC-ND) licence. This licence only allows you to download this work and share it with others as long as you credit the authors, but you can't change the article in any way or use it commercially. More information and the full terms of the licence here: <https://creativecommons.org/licenses/>

**Takedown**

If you consider content in White Rose Research Online to be in breach of UK law, please notify us by emailing [eprints@whiterose.ac.uk](mailto:eprints@whiterose.ac.uk) including the URL of the record and the reason for the withdrawal request.



[eprints@whiterose.ac.uk](mailto:eprints@whiterose.ac.uk)  
<https://eprints.whiterose.ac.uk/>

# Extraction of Uranium from Non-Saline and Hypersaline Conditions Using Iminodiacetic Acid Chelating Resin Purolite S930+

J. T. M. Amphlett<sup>a</sup>, C. A. Sharrad<sup>a</sup>, M. D. Ogden<sup>b</sup>

<sup>a</sup> School of Chemical Engineering and Analytical Science, The University of Manchester, Oxford Road, Manchester, M139PL

<sup>b</sup> Separations and Nuclear Chemical Engineering Research (SNUCER), Department of Chemical and Biological Engineering, The University of Sheffield, Mappin Street, Sheffield, S13JD

\*Corresponding author's email: james.amphlett@manchester.ac.uk

## Abstract

Uptake behaviour of uranium from aqueous, acidic sulfate and chloride media on iminodiacetic acid chelating resin Purolite S930+ has been studied. Experiments have followed  $\text{UO}_2^{2+}$ ,  $\text{Cu}^{2+}$  and  $\text{Fe}^{3+}$  uptake behaviour with respect to acidic and ionic media type and concentration. Uptake suppression of all metals was observed at  $[\text{H}^+] > 0.1 \text{ M}$  sourced from  $\text{H}_2\text{SO}_4$  and  $\text{HCl}$ . In contrast, significant uptake of  $\text{Fe}^{3+}$  was observed from solutions with  $[\text{HCl}] > 2 \text{ M}$ . Suppression of  $\text{UO}_2^{2+}$  uptake (up to 15%) was observed upon increasing  $[\text{SO}_4^{2-}]$  to 4 M, whilst negligible  $\text{UO}_2^{2+}$  uptake suppression was observed with  $[\text{Cl}^-]$  up to 6 M. The impact of  $\text{Fe}^{3+}$  concentration on  $\text{UO}_2^{2+}$  extraction under hypersaline conditions ( $[\text{Cl}^-] = 22.6 \text{ g L}^{-1}$ , 0.64 M) has been studied and behaviour fit to Langmuir and Dubinin-Radushkevich isotherms. Extended X-ray absorption fine structure (EXAFS) studies have been performed to assess the effect of salinity on the uranium coordination environment on the resin and therefore the mechanism of uptake. No change in surface species was observed, with the fit species being uranyl bound by the iminodiacetic acid functional group in a tridentate motif, with an associated bidentate

sulfate group. An isotherm model based on this surface has also been derived. It has been shown that at pH 2 there is little impact of increasing chloride and sulfate concentrations on the extraction behaviour of metals onto Purolite S930+ under the conditions tested. Rather, uranium uptake is more affected by the presence of  $\text{Fe}^{3+}$  in solution. As  $[\text{Fe}^{3+}]/[\text{UO}_2^{2+}]$  is increased from 0 to 2,  $\text{UO}_2^{2+}$  uptake is reduced by up to 66% at aqueous equilibrium.

**Keywords; Uranium, iminodiacetic acid resin, chelation, ion exchange, saline, EXAFS**

## **1. Introduction**

Uranium mines consume vast quantities of water, and many of these mines are located in arid regions with either poor access to fresh water or access only to lower quality (saline) water sources [1,2]. As an example, it is estimated that the Olympic Dam mine site in South Australia consumes 42 megalitres of fresh water per day, with a planned expansion of this site pushing this figure up to 200 megalitres per day [3]. This consumption puts a strain on fresh water supplies and increases the overall cost of the mining operation. The majority of this fresh water is used to extract soluble uranium from its ore, this liquor is then treated with ion exchange (IX) and/or solvent extraction (SX) processes as part of the milling strategy. The use of untreated bore water and/or seawater instead of fresh water in these extraction steps may address both the environmental and economic issues of using such large quantities of fresh water. However, if such waters are used in uranium extractions, the effect of  $\text{Cl}^-$  on the chemistry of the system must be fully understood. For the purposes of this paper, the  $\text{Cl}^-$  concentrations have been classified into three categories (with respect to liquors used in common uranium IX processes), conventional, saline and hypersaline liquors, as outlined in the schematic diagram (Figure 1) below.

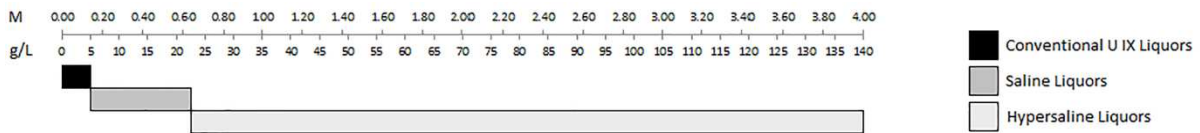


**Figure 1. Chloride concentrations in Saline and Hypersaline liquors.**

After a uranium ore has been mined, screened and crushed it undergoes leaching. This leaching process involves the solubilising of uranium to produce a pregnant leach liquor (PLL). The leach liquor used depends on the chemical makeup of the ore, but it generally employs sulfuric acid as it is more environmentally friendly than hydrochloric or nitric acid. A carbonate leach can be used if the ore consumes large amounts of acid. Ores containing tetravalent uranium need an oxidant, commonly sodium chlorate or manganese dioxide, to produce soluble hexavalent uranium which can be sent for further processing. Extraction of uranium from the PLL most commonly employs IX or SX, although nanofiltration has seen some use [4]. Ideally, the extraction medium, whether SX or IX, will selectively remove the uranium from the PLL. Therefore the choice of extractant depends heavily upon the chemistry of the PLL. The development of new extraction processes that are more tolerant to the presence of  $\text{Cl}^-$  may allow greater flexibility in the composition of the PLL, thus allowing the use of lower quality waters relative to fresh water.

Although SX is the major workhorse technology for uranium recovery there are still some general drawbacks to this process [5,6]. These include the need for an extractant molecule soluble in the organic phase, potential for solvent loss, phase disengagement in multiple contact stages, third phase formation and the generation of large volumes of secondary organic waste. IX processes, as the sorbent is solid, remove all of the difficulties of handling large volumes of organic solvent. They also often have faster kinetics than SX systems and are more effective when extracting uranium at lower concentrations [6].

The majority of uranium processing circuits are sulfate-based [7]. Processes employing IX resins for the separation/concentration of uranium typically use anion exchange resins with strong base (SBA) functional groups [8]. Those employing SX generally use long chain tertiary amines as

extractants [9]. Both techniques are sensitive to the presence of  $\text{Cl}^-$  in solution, which causes suppressed uranium uptake. Similarly to IX resins, it has been shown that tertiary amines in SX can work via an IX mechanism [10]. In both cases the suppression is due to the decreased exchange of the uranium-sulfate species due to competing  $\text{Cl}^-$  [9,11]. This is compounded by the increased exchange of iron and other impurity elements. This reduced  $\text{UO}_2^{2+}$  affinity in high saline conditions can be overcome in IX systems by the application of a chelating resin. Functionalities on the resin surface employ the chelate effect through multidentate coordination, forming thermodynamically stable complexes. In this paper the application of an iminodiacetic acid (IDA) chelation resin, Purolite S930+, to the extraction of uranium from simulant uranium process liquors has been explored. Though there are many examples of effective, novel sorbents for uranium, including layered silicates, nanocomposites, functionalised chitosan and functionalised silica (among numerous others), the Purolite S930+ resin has been selected due to its commercial availability and therefore relative ease of implementation into a traditional uranium recovery process [12–15]. The iminodiacetic acid functionality has been specifically chosen due to the fact that it offers both a strong acid uranium elution option, as  $\text{H}^+$  can effectively compete with uranium at low pH, and chelation strength usually increases with high ionic strength [16].

## **2. Experimental**

### **2.1 Reagents and Stock Solutions**

For all experimental studies, the commercially available chelating IX resin, Purolite S930+, was directly supplied by Purolite. The general specification data for this resin and other commercial equivalents, for comparative purposes, are given in Table 1 [17]. Prior to experimentation, the S930+ resin was preconditioned by contacting  $1 \text{ mol L}^{-1}$  HCl or  $\text{H}_2\text{SO}_4$  at a resin volume:acid volume ratio of 1:10 on an orbital shaker for 24 hrs at room temperature. The resin was then washed three times with 3 bed volumes (BV) of deionised water (18 M $\Omega$ ) before use. The structure of the IDA functionality of Purolite S930+ resin is given in Figure 2.

All solutions used in loading experiments were prepared using deionised water (18 MΩ) and analytical grade reagents. These uptake solutions were formulated to simulate a uranium leach liquor by the dissolution of metallic cation species commonly found in these liquors, in their sulfate form. For studies assessing the effect of iron, Fe<sup>3+</sup> was added in molar ratios of 1 and 2 relative to [UO<sub>2</sub><sup>2+</sup>] (Table 2).

**Table 1. Manufacturer Specifications Purolite S930+ and similar resins.**

	<b>Purolite S930+</b>	<b>Chelex 100</b>	<b>Amberlite IRC748</b>	<b>Lewatit TP208</b>
Type	Macroporous, weak acid chelating	Weak acid cation, chelating	Weak acid chelating	Weak acid cation, chelating
Functionality	Iminodiacetic acid	Iminodiacetic acid	Iminodiacetic acid	Iminodiacetic acid
Capacity / meq mL <sup>-1</sup>	2.9	0.4	1.35	2.5
Particle size / μm	425 -1000	150 - 300	300 - 1100	650
Moisture content / %	52 - 60 (Na form)	-	60 - 65 (Na form)	58 – 64 (delivery form)

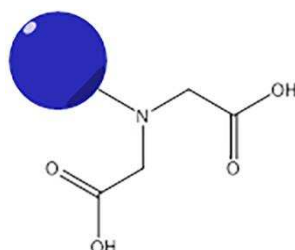


**Figure 2. Functionality of Purolite S930+ resin.**

**Table 2. Composition of Simulant Liquor used for Loading Isotherms.**

Element	Concentration / M
Ca <sup>2+</sup>	0.013
K <sup>+</sup>	0.034
Mg <sup>2+</sup>	0.019
Na <sup>+</sup>	0.724
Fe <sup>3+</sup>	0 – 0.008
UO <sub>2</sub> <sup>2+</sup>	0.0002 - 0.004

## 2.2. Batch extractions from sulfate and chloride media

All batch extractions as a function of acid concentration were carried out as single contacts with 2 mL of wet settled resin (WSR) contacted with 50 mL of aqueous simulant feed. The addition of

either NaCl or (NH<sub>4</sub>)<sub>2</sub>SO<sub>4</sub> to increase Cl<sup>-</sup> or SO<sub>4</sub><sup>2-</sup> levels in the simulant feed was carried out as part of the simulant feed production to prevent increases in experimental solution volume. UO<sub>2</sub><sup>2+</sup>, Cu<sup>2+</sup> and Fe<sup>3+</sup> were spiked into the solution at 0.42, 1.57 and 1.79 mM, respectively (100 ppm of each metal). The resin and aqueous feed were continuously mixed for a period of 24 hours at room temperature on an orbital shaker, whereafter a sample was taken to determine individual metal ion concentrations by ICP-AES (Perkin-Elmer Optima 5300 dual view). Measurements of solution pH were conducted using a silver/silver chloride reference electrode calibrated from pH 1-13 using buffers. Under highly acidic conditions (pH < 1), acid content was determined by titration with standardised alkali solution. Distribution coefficients ( $K_D$  - the weighted distribution of the analyte) were calculated using Eq.1:

$$K_D = \left( \frac{C_i - C_e}{C_e} \right) \times \frac{V_{aq}}{m_{resin}} \quad \text{Eq.1}$$

where  $C_i$  is the initial aqueous concentration of the analyte before contact (M),  $C_e$  is the aqueous concentration of the analyte at equilibrium (M),  $V_{aq}$  is the volume of the aqueous phase (mL) and  $m_{resin}$  is the dry mass of the resin (g). The extraction percentage ( $E_{\%}$ ) was calculated using Eq. 2.

$$E_{\%} = \frac{C_i - C_e}{C_e} \times 100 \quad \text{Eq.2}$$

### 2.3. Determination of loading isotherms under increasingly saline conditions

All loading isotherms were carried out as single contacts by mixing preconditioned S930+ resin (2 mL<sub>WSR</sub>) with aqueous simulant feed (50 mL). The same simulant leach liquor described previously in section 2.2 was used, but with the uranyl concentration varied and sodium chloride added to give a Cl<sup>-</sup> concentration of 0.64 M (22.6 g L<sup>-1</sup>). The resin and aqueous feed were continuously mixed for a period of 24 hours at room temperature. The data were fitted to Langmuir (Eq.3) and Dubinin-Radushkevich (D-R) (Eq.4) isotherm models [18]. The fitting was carried out by using the function

fitting builder and non-linear curve fitting in OriginPro 2015. Errors were calculated using OriginPro 2015 at a 95% confidence interval.

$$q_e = \frac{q_m b C_e}{1 + b C_e} \quad \text{Eq.3}$$

$$q_e = q_m e^{-B_{DR} \left[ RT \ln \left( 1 + \frac{1}{C_e} \right) \right]^2} \quad \text{Eq.4}$$

$B_{DR}$  = Dubinin-Radushkevich isotherm constant,  $\text{mol}^2 \text{J}^{-2}$

$C_e$  = Solution phase metal ion concentration at equilibrium,  $\text{mol L}^{-1}$

$b$  = Langmuir isotherm constant,  $\text{L mol}^{-1}$

$T$  = Absolute temperature, K

$R$  = Universal gas constant,  $8.314 \text{ J mol}^{-1} \text{ K}^{-1}$

$q_e$  = Solid phase metal ion concentration at equilibrium,  $\text{mol L}_{\text{WSR}}^{-1}$

$q_m$  = Monolayer saturation capacity,  $\text{mol L}_{\text{WSR}}^{-1}$

## 2.4. EXAFS experiments on loaded resins

Uranium  $L_{III}$ -edge EXAFS spectra were recorded in transmission mode on beamline B18 at the Diamond Light Source operating in a 10 min top-up mode with a ring current of 299.6 mA and an energy of 3 GeV. The radiation was monochromated with a Si(111) double crystal, and harmonic rejection was achieved through the use of two platinum-coated mirrors operating at an incidence angle of 7.0 mrad. The monochromator was calibrated using the K-edge of an yttrium foil, taking the first inflection point in the Y-edge as 17038 eV. Uptake on Purolite S930+ resin was performed from a uranium sulfate solution at pH 3 (adjusted with  $\text{H}_2\text{SO}_4$ ), with a uranium concentration of  $1 \text{ g L}^{-1}$ . Samples were homogenised by grinding the resin into a fine powder prior to uptake. This avoids the incorporation of artefacts into the data due to the inefficient packing of spherical resin beads. Loaded

resin (2 mL<sub>WSR</sub>) was added to a cryo-tube before being vacuum sealed in plastic. The samples were left this way during measurement. Multiple spectra from the same system were combined, background subtracted and normalised using the software package Athena [19]. Spectrum simulations and fits were done using the FEFF database through the software package Artemis [19,20].

## 3 Results

### 3.1 Batch extraction from sulfate and chloride media

#### 3.1.1 Batch extraction from sulfate media

The extraction of uranyl, copper(II) and iron(III) from sulphuric acid media as a function of increasing acid concentration over 24 hours at room temperature is shown in Figure 3, while the influence of  $[\text{SO}_4^{2-}]$  on the same system fixed at pH 2 is shown in Figure 4.

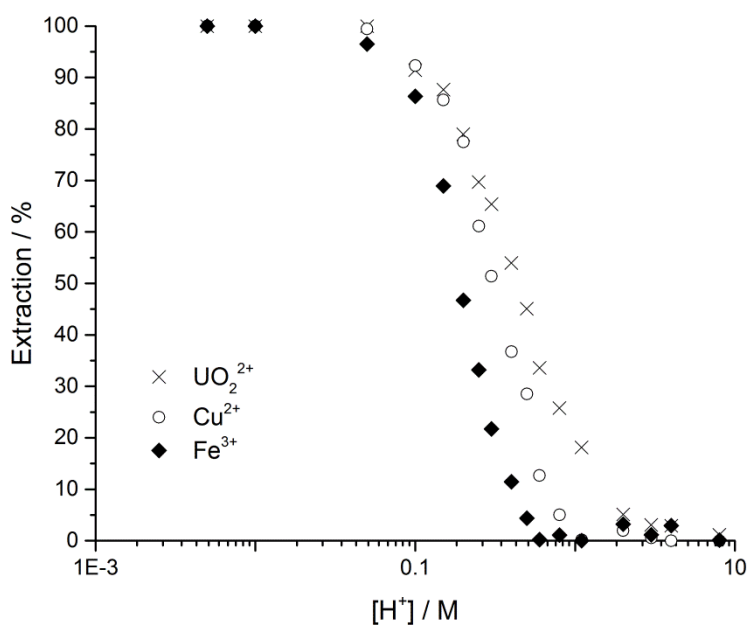
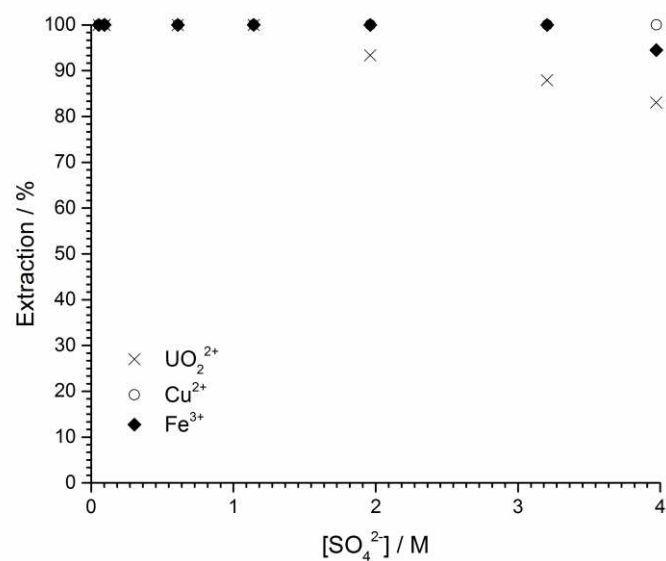
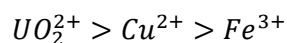


Figure 3. Extraction of  $\text{UO}_2^{2+}$ ,  $\text{Cu}^{2+}$  and  $\text{Fe}^{3+}$  by Purolite S930+ as a function of pH in  $\text{H}_2\text{SO}_4$  media at room temperature.



**Figure 4. Extraction of  $UO_2^{2+}$ ,  $Cu^{2+}$  and  $Fe^{3+}$  by Purolite S930+ as a function of sulfate concentration, at pH 2 and room temperature.**

Generally, as the concentration of  $H_2SO_4$  increases, the uptake of all tested species is suppressed. All metal ion species are extracted completely at  $[H^+] < 0.04$  M, with  $UO_2^{2+}$  and  $Cu^{2+}$  having the highest affinity for uptake as this acid concentration is exceeded. As a function of sulfuric acid concentration it is clear that  $UO_2^{2+}$  is the most strongly extracted metal species of those studied in this work (Figure 3). Under industrially relevant conditions (pH 0.5 – 3 /  $[H^+] = 0.6 – 0.05$ ) the extraction trend is as follows:



At very high sulfate concentrations ( $> 1$  M) and a fixed pH 2 (Figure 4), the extraction of  $UO_2^{2+}$  by the S930+ resin is slightly suppressed when compared with that observed for  $Cu^{2+}$  and  $Fe^{3+}$  with both metal ions being at least nearly extracted entirely from solution. Although, the extent of uranyl extraction is still above 80 % from solutions of 4 M  $SO_4^{2-}$  (pH 2).

The greatest degree of metal ion uptake suppression for S930+ resin occurs by increasing the concentration of hydrogen ions in solution. The IX equilibrium favors the IDA functionality remaining protonated, as per Le Chatelier's principle. This idea is corroborated by the suppression of metal ion uptake by sulfate not being observed until sulfate concentration exceeds 1 M (Figure 4). The lowest sulfate concentration, when sourced from  $(\text{NH}_4)_2\text{SO}_4$ , required to give an observable suppression of uranyl uptake is  $\sim 50$  times more than that observed when sulfate is sourced from  $\text{H}_2\text{SO}_4$  (Figure 3, Figure 4). Uptake suppression from sulfate occurs due to competition between the formation of uranyl-sulfate and uranyl-IDA species. A large  $[\text{SO}_4^{2-}]$  is needed to suppress uranyl recovery, which infers that the uranyl cation binds much more strongly to IDA than to aqueous  $\text{SO}_4^{2-}$  anions. This is most likely due to the increased thermodynamic stability via a chelation mechanism.

### 3.1.2 Batch extraction from chloride media

The extraction of  $\text{UO}_2^{2+}$ ,  $\text{Cu}^{2+}$  and  $\text{Fe}^{3+}$  from HCl media as a function of increasing acid concentration over 24 hours at room temperature is shown in Figure 5. The extraction of metal ions as a function of increasing  $\text{Cl}^-$  ion concentration at pH 2 is shown in Figure 6.

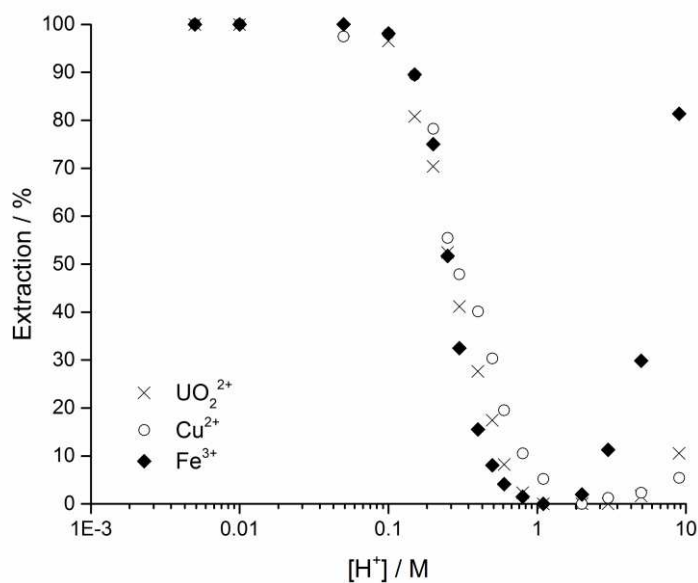
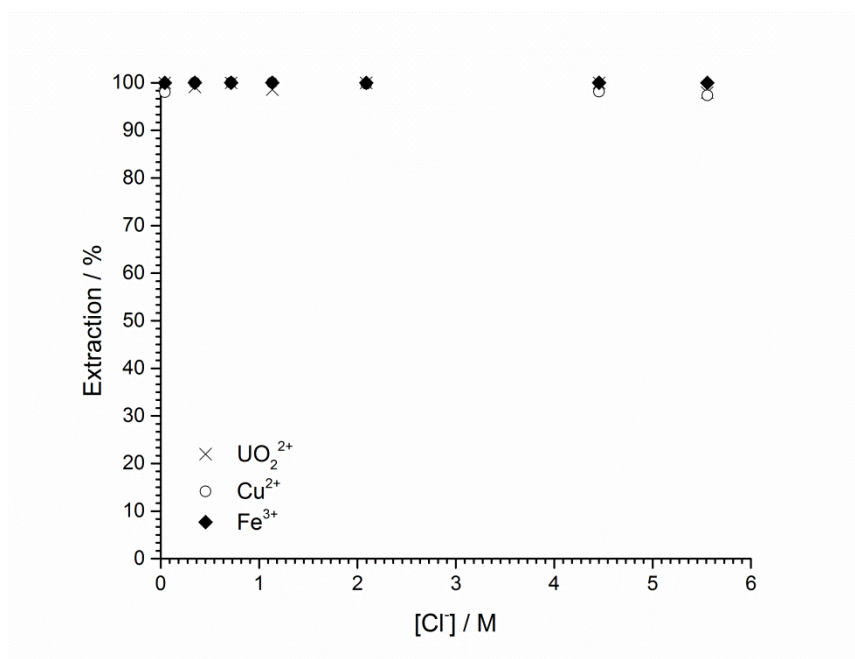


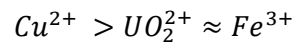
Figure 5. Extraction of  $\text{UO}_2^{2+}$ ,  $\text{Cu}^{2+}$  and  $\text{Fe}^{3+}$  by Purolite S930+ as a function of pH in HCl media at room temperature.



**Figure 6. Extraction of  $\text{UO}_2^{2+}$ ,  $\text{Cu}^{2+}$  and  $\text{Fe}^{3+}$  by Purolite S930+ as a function of chloride concentration at pH 2 in HCl media at room temperature.**

Negligible metal ion uptake suppression is observed for  $[\text{HCl}] < 0.1 \text{ M}$ . For HCl concentrations between 0.1 and 1 M suppression of all metal ion species studied is seen to such an extent that  $< 2\%$  extraction is obtained for each of the metal ions between 1 and 2 M HCl. When  $[\text{HCl}]$  is increased to above 1 M the near complete uptake suppression for  $\text{UO}_2^{2+}$  and  $\text{Cu}^{2+}$  by S930+ is maintained. When metal ion uptake suppression occurs for S930+ resin in HCl media, it is due to the increased solution  $[\text{H}^+]$  shifting the chemical equilibrium so as to prevent  $\text{H}^+$  dissociation from the IDA moiety, as described for the equivalent  $\text{H}_2\text{SO}_4$  dependency studies in section 3.1.1. However,  $\text{Fe}^{3+}$  undergoes significantly elevated levels of extraction with increasing HCl concentration above 2 M. This increase in  $\text{Fe}^{3+}$  extraction is most likely due to an anion exchange mechanism with the extraction of  $[\text{FeCl}_4]^-$  by positively charged IDA groups on the surface of the resin. This mechanism has been reported before during the SX of iron from chloride media using *N,N'*-Dimethyl-*N,N'*-dibutylmalonamide and in  $\text{Fe}^{3+}$  IX

processes at high [HCl] [21–23]. The affinities of the studied metal ions to S930+ exhibit the following overall trend when [HCl] < 1 M:



At pH 2 and increasing Cl<sup>-</sup> concentration (up to 6 M), there is minimal suppression in uptake of all the studied metal ions in this work by S930+ (Figure 6).

## 3.2. Determination of loading behaviour under saline conditions

### 3.2.1 The Effect of Fe<sup>3+</sup> concentration on UO<sub>2</sub><sup>2+</sup> loading behaviour under hypersaline conditions

The effect of increasing the Fe<sup>3+</sup> to UO<sub>2</sub><sup>2+</sup> ratio in hypersaline conditions (22.6 g L<sup>-1</sup> Cl<sup>-</sup>) at pH 2 on the uptake of UO<sub>2</sub><sup>2+</sup> on Purolite S930+ is shown in Figure 7. It is observed that increasing [Fe<sup>3+</sup>] suppresses the extraction of UO<sub>2</sub><sup>2+</sup> by Purolite S930+. Generally, the Langmuir model provided better fits of the data than those from the Dubinin-Radushkevich model, however, the latter model did produce a slightly better R<sup>2</sup> value for the fit of the data from the experiments where [Fe<sup>3+</sup>]/[UO<sub>2</sub><sup>2+</sup>] = 1. The Dubinin-Radushkevich model also largely overestimates the maximum uranium loading capacities. Fitting parameters for each model applied to the loading of uranyl onto S930+ in the presence of Fe<sup>3+</sup> are presented in Table 3. The Langmuir constant (b) is seen to increase with increasing [Fe<sup>3+</sup>]/[UO<sub>2</sub><sup>2+</sup>], with the Dubinin-Radushkevich constant (B<sub>DR</sub>) doing the inverse. The suppression of uptake can be seen as a reduction in maximum IX capacity for UO<sub>2</sub><sup>2+</sup> with increasing [Fe<sup>3+</sup>]/[UO<sub>2</sub><sup>2+</sup>] ratio, as shown by q<sub>m</sub> which is the monolayer saturation capacity for UO<sub>2</sub><sup>2+</sup> in mol L<sub>WSF</sub><sup>-1</sup>. It can be assumed that the difference in q<sub>m</sub> between systems with and without Fe<sup>3+</sup> equates to the amount of IX sites on the resin occupied by Fe<sup>3+</sup>.

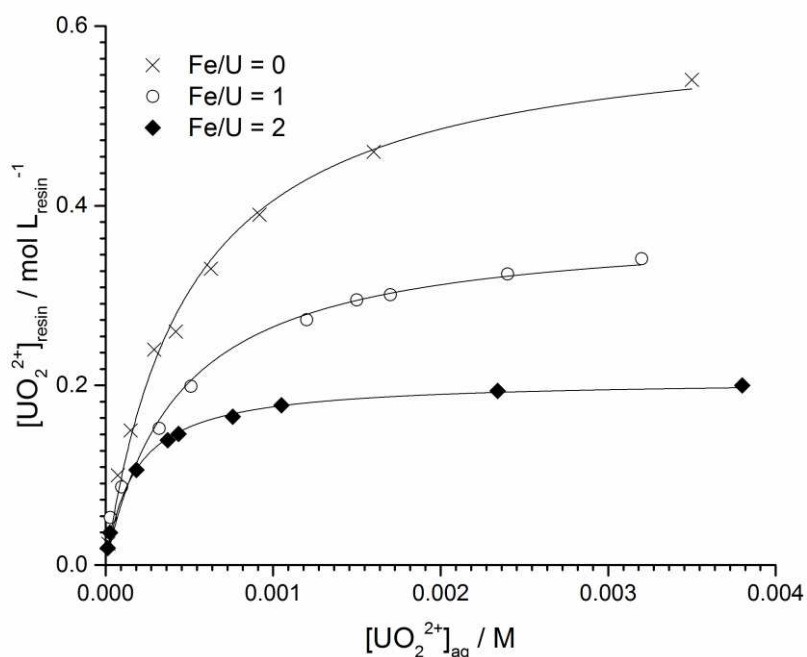


Figure 7.  $\text{UO}_2^{2+}$  uptake onto Purolite S930+ with  $[\text{Fe}^{3+}]/[\text{UO}_2^{2+}] = 0, 1$  and  $2$ . Langmuir fitting is shown by black lines.

Table 3. Langmuir and Dubinin-Radushkevich isotherm parameters obtained from fits of data from uranyl loading onto Purolite S930+ in the presence of increasing  $\text{Fe}^{3+}$  concentrations

Loading Conditions	Langmuir			Dubinin-Radushkevich		
	$b$ ( $\times 10^3$ )	$q_m$ / mol $\text{L}_{\text{WSR}}^{-1}$	$R^2$	$B_{\text{DR}}$ ( $\times 10^{-9}$ )	$q_m$ / mol $\text{L}_{\text{WSR}}^{-1}$	$R^2$
Fe/U = 0	$2.043 \pm 0.167$	$0.604 \pm 0.018$	0.993	$4.211 \pm 0.275$	$1.342 \pm 0.111$	0.981
Fe/U = 1	$2.320 \pm 0.341$	$0.379 \pm 0.015$	0.982	$3.913 \pm 0.200$	$0.809 \pm 0.045$	0.991
Fe/U = 2	$5.834 \pm 0.432$	$0.206 \pm 0.003$	0.996	$2.744 \pm 0.347$	$0.377 \pm 0.042$	0.939

### 3.2.2. EXAFS

$\text{U L}_{\text{III}}$ -edge EXAFS data were obtained of Purolite S930+ samples after  $\text{UO}_2^{2+}$  loading from non-saline and hypersaline media. The normalised EXAFS decay spectra are displayed in Figure 8. Collected spectra appear to show that there is no effect of  $\text{Cl}^-$  concentration upon surface speciation as the spectra plotted in  $k$ -space and  $R$ -space are almost identical (Figure 9).

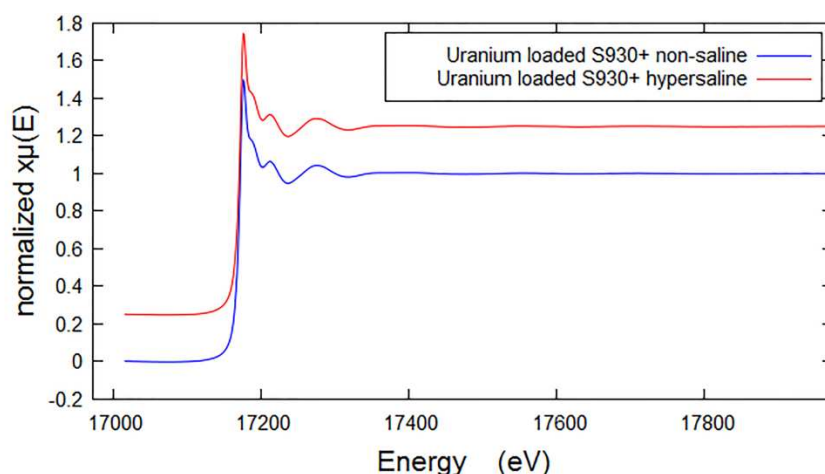


Figure 8. Normalised EXAFS decay spectra of Purolite S930+ loaded with  $UO_2^{2+}$  in non-saline and hypersaline conditions.

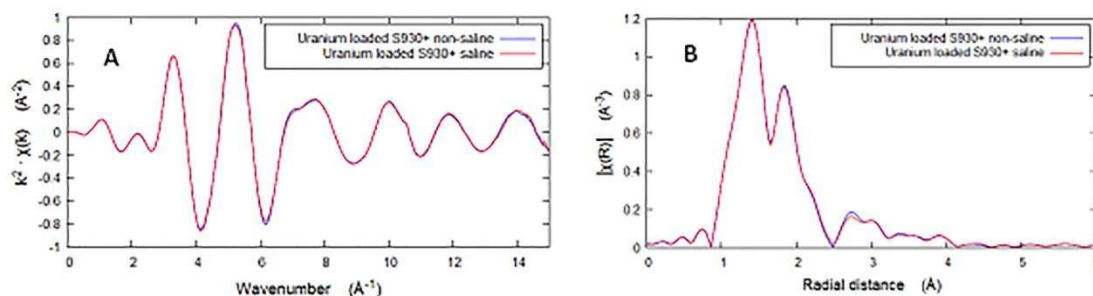


Figure 9. EXAFS spectra of Purolite S930+ loaded with  $UO_2^{2+}$  in K-space (A) and R-space (B).

## 4 Discussion

### 4.1 Batch extraction from sulfate and chloride media

The point at which 50% extraction occurs for the  $Fe^{3+}$ ,  $Cu^{2+}$ , and  $UO_2^{2+}$  as a function of  $H^+$  concentration ( $[H^+]_{50}$  and  $pH_{50}$ ) in hydrochloric and sulfuric acid media can be used as an indicator of the strength of the interaction between the resin and metal ion (Table 4). The point at which 50% extraction occurs is predicted by polynomial fitting of the closest five data points to 50% extraction which gives  $R^2 > 0.9990$  for all data sets. From the data in Table 4 it can be seen that the 50% extraction values in HCl media cannot be grouped by electrostatics, with very similar values for all metal ions tested. In  $H_2SO_4$  media there is a clear trend of decreasing  $[H^+]_{50}$  values as  $z/IR$  increases. This infers

that the interaction between the metal ions and the IDA functionality is not purely governed by electrostatics. It is likely that the strength of the interaction between metal and resin is affected by the size of the metal cation and how well it fits into the chelate ring. As metal ionic radius decreases, it is more difficult for the IDA group to bind in a tridentate fashion as the binding cavity size will need to be reduced, producing strain in the chelate ring and making binding less energetically favorable.

**Table 4. The 50% extraction point in hydrochloric and sulfuric acid media by Purolite S930+.**[24,25]

Species	z	Ionic Radius / Å	z/IR	HCl Media		H <sub>2</sub> SO <sub>4</sub> Media	
				[H <sup>+</sup> ] <sub>50</sub>	pH <sub>50</sub>	[H <sup>+</sup> ] <sub>50</sub>	pH <sub>50</sub>
Fe <sup>3+</sup>	3	0.55	5.45	0.25	0.60	0.20	0.70
Cu <sup>2+</sup>	2	0.73	2.74	0.28	0.55	0.31	0.51
UO <sub>2</sub> <sup>2+</sup>	2	1.40	1.43	0.26	0.59	0.45	0.35

## 4.2. Determination of loading behaviour under hypersaline conditions

Data for uranium loading isotherms with increasing concentrations of [Fe<sup>3+</sup>] were collected using hypersaline conditions (Cl<sup>-</sup> = 22.6 g L<sup>-1</sup>, 0.64 M) at pH 2. At this pH regime the H<sup>+</sup> concentration does not cause any uranyl uptake suppression (Figures 5 & 6). One of the parameters that can be calculated from the Dubinin-Radushkevich model is the mean free energy of sorption, which can give an indication of the type of mechanism employed in the extraction. These values are presented in Table 5. Mean free energy of sorption values are seen to increase with increasing [Fe<sup>3+</sup>]/[UO<sub>2</sub><sup>2+</sup>], indicating a stronger interaction between the uranyl cation and the IDA moiety at higher Fe<sup>3+</sup> concentrations. This is the inverse of the relationship between [Fe<sup>3+</sup>]/[UO<sub>2</sub><sup>2+</sup>] and maximum loading capacity obtained using the Langmuir model. The effect of increasing molar ratio ([Fe<sup>3+</sup>]/[UO<sub>2</sub><sup>2+</sup>]) in the IX capacity towards uranyl under experimental conditions is shown in Figure 10.

**Table 5. Mean free energy of sorption values and uranyl loading capacities for uranium loading at  $[Fe^{3+}]/[UO_2^{2+}]$  values of 0, 1 and 2.**

$[Fe^{3+}]/[UO_2^{2+}]$	Mean free energy of sorption / $kJ\ mol^{-1}{}^A$	$q_m / mol\ L_{WSR}^{-1}{}^B$
0.0	$10.90 \pm 0.36$	$0.604 \pm 0.018$
1.0	$11.30 \pm 0.29$	$0.379 \pm 0.015$
2.0	$13.50 \pm 0.85$	$0.206 \pm 0.003$

<sup>A</sup>Calculated using the Dubinin-Radushkevich model. <sup>B</sup>Calculated from the Langmuir model.

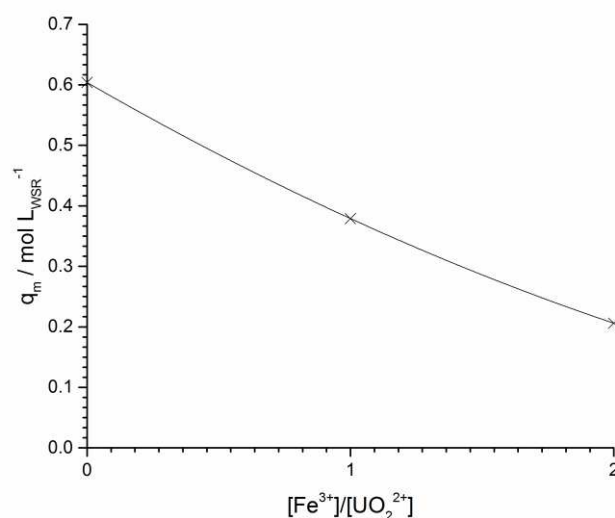


**Figure 10.  $UO_2^{2+}$  saturation capacity ( $mol\ L_{WSR}^{-1}$ ) with increasing  $[Fe^{3+}]/[UO_2^{2+}]$  molar ratio from Langmuir isotherm model fitting. Fitted line is to guide the eye.**

The suppression of uranyl uptake by Purolite S930+ upon increasing  $[Fe^{3+}]$  occurs due to competition for uptake sites on the resin surface between the two species. The observed results infer an increased affinity for  $Fe^{3+}$  by S930+ when compared with  $UO_2^{2+}$ . Formation constants ( $\log_{10}\beta$ ) for the 1:1  $Fe^{3+}$  or  $UO_2^{2+}$  complex with iminodiacetic acid in aqueous solution have been reported as 10.72 and 9.90, respectively [26,27]. This higher formation constant for the  $Fe^{3+}$ -IDA complex suggests that Purolite S930+ will form stronger complexes with  $Fe^{3+}$ , agreeing with the collected experimental data.

This reduction in  $\text{UO}_2^{2+}$  recovery would be problematic in uranium processing circuits, so  $[\text{Fe}^{3+}]$  would need to be controlled. This could be achieved by adjusting the pH to 3, promoting iron precipitation, or  $\text{Fe}^{3+}$  could be chemically reduced to  $\text{Fe}^{2+}$ . An alternative to those methods would be an initial extraction step in concentrated HCl media, promoting the removal of  $[\text{FeCl}_4^-]$ , followed by increasing the pH and extracting the uranium. However, this system would increase plant acid consumption, so it may not be suitable.

### **4.3. Determination of surface speciation**

Purolite S930+ is marketed as a chelation ion exchanger, and fits of the EXAFS data obtained from uranyl loaded S930+ to molecular species were conducted with this in mind. Uranyl is a 2+ cation, therefore according to charge balance, two positive charges must be transferred from the IDA moiety into the aqueous phase for uranyl to bind to IDA. The  $\text{pK}_a$  values of free IDA in aqueous solution suggest that one acetic acid group will be deprotonated under experimental conditions used to load the uranyl onto the resin for the EXAFS samples, meaning the two  $\text{H}^+$  ions which are transferred from the IDA moiety will most likely be from the protonated acetate group and from the protonated nitrogen atom [28]. This alludes to a possible mechanism where the IDA binds to uranyl in a tridentate fashion. Modelling of the uranium coordination environment was conducted incorporating two axial oxygen atoms, two equatorial oxygen atoms and one equatorial nitrogen atom. For the rest of the equatorial region, numbers of oxygen atoms were varied to find the best fit. The same fitting methodology was applied to data collected in both non-saline and hypersaline environments. The addition of scattering paths associated with  $\text{Cl}^-$  groups was not seen to improve fitting parameters in hypersaline fits. Fits are presented in R-space and K-space (Figure 11). Fitting parameters are shown in Table 6, with atomic parameters from the fit shown in Table 7.

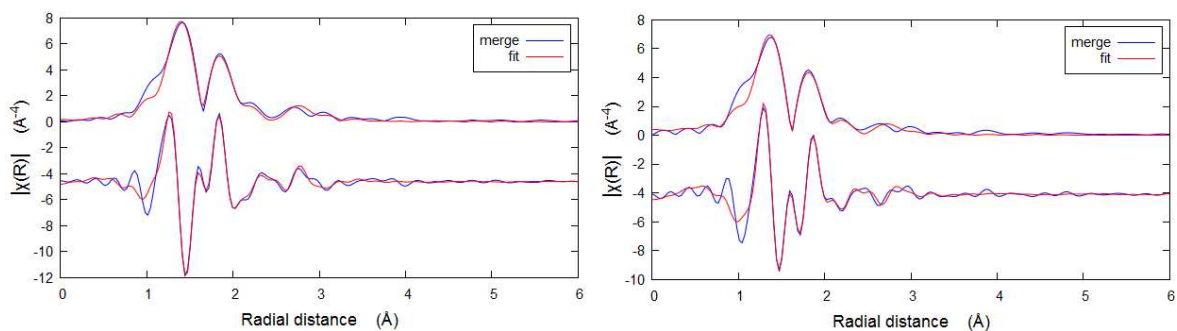


**Figure 11. U L<sub>III</sub>-edge EXAFS fits of uranyl loaded Purolite S930+ from non-saline (left) and hypersaline (right) environments.**

**Table 6. Fitting parameters produced from U L<sub>III</sub>-edge EXAFS data fitting of uranyl loaded Purolite S930+ from non-saline and hypersaline environments.**

	Non-Saline	Hypersaline
R-factor	0.0168	0.0170
$\chi_{\text{red}}^2$	968.863	2602.083
Amp	1.071	0.945
dE <sub>0</sub>	0.567	0.862

**Table 7. Atom parameters from U L<sub>III</sub>-edge EXAFS data fitting of uranyl loaded Purolite S930+ from non-saline and hypersaline environments (*O<sub>axial</sub>* are axial oxygen atoms, *O<sub>eq</sub>* are oxygen atoms associated with the IDA moiety or aqueous species, *N* is a resin based nitrogen atom and *S* is a sulfur atom associated with a sulfate group.)**

	Non-Saline			Hypersaline		
	N	R / Å	$\sigma^2$	N	R / Å	$\sigma^2$
O <sub>ax</sub>	2	1.78675	0.0028	2	1.78834	0.00234
O <sub>eq</sub>	2	2.41479	0.00194	4	2.36268	0.00527
O <sub>eq</sub>	2	2.31017	0.00248	-	-	-
N	1	2.54725	0.00163	1	2.53526	0.00034
S	1	3.10699	0.00686	1	3.12785	0.00899

Best fits were produced for a five coordinate uranyl in the equatorial plane. The IDA acts as a tridentate chelating ligand (Figure 12) with the uranyl coordination environment about the equatorial plane completed by two oxygen atoms. The tridentate motif provided by IDA has been observed in the solid state previously by Jiang *et al.* [29], though U-N distances are slightly greater than those seen in these EXAFS spectra, which can be attributed to the differences between aqueous and solid systems. The remaining oxygen donor atoms in the uranyl equatorial plane may be associated with either water, hydroxyl groups, sulfate groups or a mixture of all three as these oxygen donors are indistinguishable given the experiments performed, and the potentially transient nature of these ligands with uranyl in an aqueous environment. The inclusion of a sulfur atom (or atoms) in a secondary uranyl coordination sphere for the EXAFS fits was attempted in order to ascertain if these remaining oxygen donors are sourced from sulfate. A way of assessing the statistical significance of the addition of another scattering path to an EXAFS fit is by using a variation on the F-test [30,31]. This method produces a confidence value for the addition of the extra scattering path using goodness of fit parameters. Equations 6-8 show how the confidence interval is calculated, where F is the result of the F-test,  $R_1$  and  $R_0$  are the R-factors for the worse and better fits, respectively, n is the number of independent points in the fit, m is the number of variables used in the fit, b is the difference in the number of parameters used in fits of  $R_1$  and  $R_0$  (known as the dimension of the fit),  $I_x$  is the incomplete beta function and  $\alpha$  is the confidence level. A confidence level of 65% or greater suggests that the addition of the extra scattering path produces a statistically significant improvement to the fit. However, it is generally accepted that to be truly confident that this addition is a statistically significant improvement, a value of 95% or higher is required.

$$F = \frac{(R_1^2 - R_0^2)/b}{R_0^2/(n-m)} = \left[ \left( \frac{R_1}{R_0} \right)^2 - 1 \right] \times \frac{n-m}{b} \quad \text{Eq.6}$$

$$\alpha = 1 - I_X\left(\frac{n-m}{2}, \frac{b}{2}\right) \quad \text{Eq.7}$$

$$X = \left(\frac{n-m}{n-m+bF}\right) \quad \text{Eq.8}$$

The F-test produces confidence levels of 97% and 92% for the addition of a sulfur scattering path in EXAFS fits from non-saline and hypersaline environments, respectively. This is strong evidence that there is always a sulfur atom associated with the complexed uranyl cation. The slightly lower confidence interval for the hypersaline fit suggests that the scattering path is not as important as in non-saline conditions. This may mean that the sulfate group is not associated with the uranyl complex in non-saline conditions as often as in hypersaline conditions. However, a confidence level of 92% still shows that the sulfur atom, and therefore sulfate group is almost always present in the uranyl coordination environment and is very important in the fit. This leads to the conclusion that a bidentate sulfate group is associated with the surface complex in both aqueous environments tested. This is also evidenced by the U-S interatomic distance of 3.107 and 3.129 Å from non-saline and hypersaline conditions, respectively, which agree with previously published data for bidentate sulfate coordinated to uranyl where the U-S distances are ~ 3.1 Å [32].

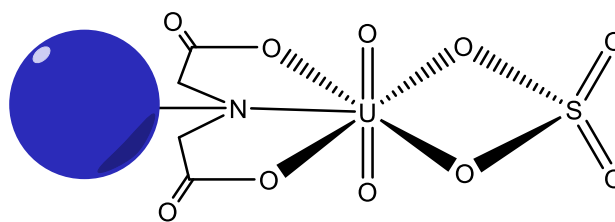
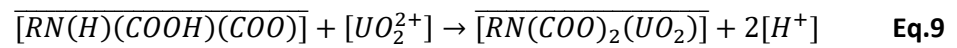


*Figure 12. Schematic representation of uranyl bound to Purolite S930+.*

### 4.3. Isotherm Derivation

An extraction mechanism for  $\text{UO}_2^{2+}$  by a Purolite S930+ has been proposed using the uranium coordination environment elucidated from the EXAFS data fits (Eq.9). This has allowed for the

derivation of an isotherm model for this system based on the mass action law (Eq.10). The parameter  $\alpha_{IDA^{2-}}$  is the fraction of the IDA moiety present in the dianionic form (Eq.11), while  $k_{1,2,3}$  are the stepwise deprotonation constants for IDA [33,34]. The full derivation is shown in the supplemental information in Appendix 1. As the IDA functionality is a triprotic system. Free IDA has the following protonation constants in aqueous:  $pK_1 = 1.77$  ( $CO_2H$ ),  $pK_2 = 2.62$  ( $CO_2H$ ) and  $pK_3 = 9.34$  ( $NHR_2$ ) [28]. We can make the assumption that it is the  $IDA^{2-}$  form that actively complexes the metal from solution due to the results of the EXAFS experiments.



$$y = \frac{k_{ex}\alpha_{IDA^{2-}}xS}{1+k_{ex}\alpha_{IDA^{2-}}x} \quad \text{Eq.10}$$

$$\alpha_{IDA^{2-}} = \frac{k_1k_2k_3}{[H^+]^3+k_1[H^+]^2+k_1k_2[H^+]+k_1k_2k_3} \quad \text{Eq. 11}$$

Model fits were performed for isotherm data with increasing  $[Fe^{3+}]/[UO_2^{2+}]$  (Table 8, Fig. 13). Maximum loading capacity is seen to decrease as  $[Fe^{3+}]$  increases. Additionally, the  $R^2$  values and  $q_m$  values predicted by the model are identical to those produced by the Langmuir isotherm. This arises as the equations are of the same form. The fit extraction equilibrium constant ( $k_{ex}$ ) is of the same order of magnitude for all values of  $[Fe^{3+}]/[UO_2^{2+}]$ . The value produced when  $[Fe^{3+}]/[UO_2^{2+}] = 2$  is around 2.5 times higher than when  $[Fe^{3+}]/[UO_2^{2+}] = 0$  and 1. This change may be due to the higher ionic strength of the aqueous solution with increasing  $[Fe^{3+}]$ .

**Table 8. Fitting parameters from the derived isotherm model.**

$[\text{Fe}^{3+}]/[\text{UO}_2^{2+}]$	$R^2$	$k_{\text{ex}} (\times 10^{13})$	$S / \text{mol L}_{\text{WSR}}^{-1}$
0	0.994	$2.5 \pm 0.2$	0.604
1	0.984	$2.9 \pm 0.4$	0.379
2	0.996	$7.2 \pm 0.5$	0.206

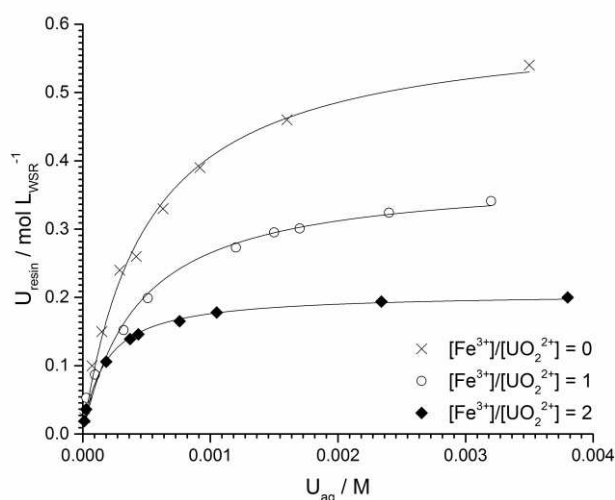


**Figure 13. Derived isotherm model fit for uranium uptake on Purolite S930+ with differing concentrations of iron.**

## 5. Conclusions

Under the conditions tested Purolite S930+ has been shown to be a viable candidate for uranium extraction under hypersaline conditions, with maximum uranyl loading capacity in hypersaline conditions being  $0.604 \text{ mol L}_{\text{WSR}}^{-1}$  ( $143.75 \text{ g L}_{\text{WSR}}^{-1}$ ). Collected data shows that  $\text{Cl}^-$  concentration has very little impact upon uranium extraction ability and mechanism. It has also been observed that increasing  $[\text{SO}_4^{2-}]$  has little impact on uranium uptake. However,  $[\text{H}^+]$  in both sulfuric and HCl media is seen to significantly suppress uranium uptake and would therefore need to be controlled and kept below 0.1 M. The presence of  $\text{Fe}^{3+}$  in solution was also seen to cause a reduction in  $\text{UO}_2^{2+}$  recovery, by as much as 66% when  $[\text{Fe}^{3+}]/[\text{UO}_2^{2+}] = 2$ .

The IDA moiety on Purolite S930+ has been shown to chelate the uranyl cation in a tridentate fashion in non-saline and hypersaline conditions through the use of EXAFS experiments. EXAFS data has been fit using crystallographic data and shows a 5-coordinate equatorial plane, with two oxygen atoms and a nitrogen atom from the IDA group and two oxygen atoms from a bidentate sulfate group. Assigning two of the oxygen atoms to a sulfate group as opposed to  $\text{OH}^-$  or  $\text{H}_2\text{O}$  was deemed correct from assessing the statistical significance of adding a U-S-U single scattering path to the fits using a variation on the F-test. This identical surface uranyl speciation in non-saline and hypersaline environments further shows the lack of impact  $\text{Cl}^-$  concentration has on uranyl uptake.

Collected data shows that the use of Purolite S930+ is clearly better than traditional SBA resins if a move to more environmentally friendly uranium mining processing circuits is to happen. It has been reported that the addition of  $2.5 \text{ g L}^{-1} \text{ Cl}^-$  to uranium process liquors can reduce extraction by up to 20%, which makes the process essentially economically unfeasible [35]. Purolite S930+ also has an advantage over other chelating resins such as those containing the aminophosphonic (Purolite S950) and mixed sulfonic/phosphonic acid (Purolite S957) functional groups as it can readily be eluted under moderately acidic conditions with  $1 \text{ mol L}^{-1} \text{ HCl}$  or  $\text{H}_2\text{SO}_4$ . The copper present in the solution system tested can be removed by pretreating the eluent with chelating IX resin Dowex M4195 which is able to form strong complexes with  $\text{Cu}^{2+}$ .

## 6. Acknowledgements

The authors would like to thank staff on beamline B18 at the Diamond Light Source, specifically Dr. Stephen Parry and Dr. Giannantonio Cibin, for their assistance with EXAFS experiments. We also thank the University of Sheffield for supplying stock uranium solutions and Purolite for supplying S930+ ion exchange resin. We acknowledge the SNUCER group at the University of Sheffield for their help with parts of this work, and Mr. Paul Lythgoe at the Manchester Analytical Geochemistry Unit (MAGU), University of Manchester, for performing ICP-AES analysis.

## 7. References

- [1] M.A. Ford, Uranium in South Africa, *J. South African Inst. Min. Metall.* 93 (1993) 37–58.  
doi:10.1111/j.1813-6982.1953.tb01589.x.
- [2] D. Lunt, P. Boshoff, M. Boylett, Z. El-Ansary, Uranium extraction: the key process drivers, *J. South. African Inst. Min. Metall.* 107 (2007) 419.
- [3] Olympic Dam Expansion, Draft Environmental Impact Statement, 2009.
- [4] M. Peacock, S. McDougall, P. Boshoff, D. Butcher, M. Ford, S. Donegan, D. Bukunkwe, Nano-filtration technology for reagent recovery, in: *ALTA Uranium-REE Sess., ALTA Metallurgical Services Publications*, Perth, 2016.
- [5] A. Taylor, *Short Course in Uranium Ore Processing*, ALTA Metallurgical Services Publications, 2016.
- [6] J. Veliscek-Carolan, Separation of actinides from spent nuclear fuel: A review, *J. Hazard. Mater.* 318 (2016) 266–281. doi:10.1016/j.jhazmat.2016.07.027.
- [7] C.R. Edwards, A.J. Oliver, Uranium processing: A review of current methods and technology, *J. Miner. Met. Mater. Soc.* 52 (2000) 12–20. doi:10.1007/s11837-000-0181-2.
- [8] E. Rosenberg, G. Pinson, R. Tsosie, H. Tutu, E. Cukrowska, Uranium remediation by ion exchange and sorption methods: A critical review, *Johnson Matthey Technol. Rev.* 60 (2016) 59–77. doi:10.1595/205651316X690178.
- [9] J.E. Quinn, D. Wilkins, K.H. Soldenhoff, Solvent Extraction of Uranium from Saline Leach Liquors Using DEHPA/Alamine 336 Mixed Reagent, *Hydrometallurgy*. 134 (2013) 74–79.
- [10] K.B. Brow, C.F. Coleman, D.J. Crouse, J.O. Denis, J.G. Moore, The use of amines as extractants for uranium from acidic sulfate liquors: a preliminary report, D. E., U.S. At. Energy Comm., Rept. ORNL-1734. (1954). doi:10.1017/CBO9781107415324.004.
- [11] K. Soldenhoff, Solvent Extraction and Ion Exchange Technologies for Uranium Recovery from Saline Solutions, in: *ALTA*, 2006.
- [12] Z. Chen, Y. Liang, D. Jia, W. Chen, Z. Cui, X. Wang, Layered silicate RUB-15 for efficient

- removal of  $\text{UO}_2^{2+}$  and heavy metal ions by ion-exchange, *Environ. Sci. Nano.* 4 (2017) 1851–1858. doi:10.1039/C7EN00366H.
- [13] W. Yao, X. Wang, Y. Liang, S. Yu, P. Gu, Y. Sun, C. Xu, J. Chen, T. Hayat, A. Alsaedi, X. Wang, Synthesis of novel flower-like layered double oxides/carbon dots nanocomposites for U(VI) and  $^{241}\text{Am(III)}$  efficient removal: Batch and EXAFS studies, *Chem. Eng. J.* 332 (2018) 775–786. doi:10.1016/j.cej.2017.09.011.
- [14] L. Zhou, H. Zou, Y. Wang, Z. Huang, Y. Wang, T. Luo, Z. Liu, A.A. Adesina, Adsorption of uranium(VI) from aqueous solution using magnetic carboxymethyl chitosan nano-particles functionalized with ethylenediamine, *J. Radioanal. Nucl. Chem.* 308 (2016) 935–946. doi:10.1007/s10967-015-4525-3.
- [15] G. Xue, F. Yurun, M. Li, G. Dezhi, J. Jie, Y. Jincheng, S. Haibin, G. Hongyu, Z. Yujun, Phosphoryl functionalized mesoporous silica for uranium adsorption, *Appl. Surf. Sci.* 402 (2017) 53–60. doi:10.1016/j.apsusc.2017.01.050.
- [16] A.E. Martell, R.S. Smith, R.J. Motekaitis, NIST critically selected stability constants of metal complexes, *NIST Stand. Ref. Database.* 8 (2004).
- [17] Purolite, Purolite Product Guide Characteristics and Applications, 2011.
- [18] K.Y. Foo, B.H. Hameed, Insights into the modeling of adsorption isotherm systems, *Chem. Eng. J.* 156 (2010) 2–10. doi:10.1016/j.cej.2009.09.013.
- [19] B. Ravel, M. Newville, *ATHENA*, *ARTEMIS*, *HEPHAESTUS*: data analysis for X-ray absorption spectroscopy using *IFEFFIT*, *J. Synchrotron Radiat.* 12 (2005) 537–541. doi:10.1107/S0909049505012719.
- [20] M. Newville, *IFEFFIT*: interactive XAFS analysis and FEFF fitting, *J. Synchrotron Radiat.* 8 (2001) 322–324.
- [21] M.C. Costa, M. Martins, A.P. Paiva, Solvent Extraction of Iron(III) from Acidic Chloride Media Using N,N'-Dimethyl-N,N'-dibutylmalonamide, *Sep. Sci. Technol.* 39 (2004) 3573–3599. doi:10.1081/SS-200036785doi.org/10.1081/SS-200036785.

- [22] Y. Marcus, The Anion Exchange of Metal Complexes - IV The Iron(III)-Chloride System, *J. Inorg. Nucl. Chem.* 12 (1958) 287–296.
- [23] A.C. Reents, F.H. Kahler, Anion Exchange Removal of Iron from Chloride Solutions, *Ind. Eng. Chem.* 47 (1955) 75–77.
- [24] R.D. Shannon, Revised effective ionic radii and systematic studies of interatomic distances in halides and chalcogenides, *Acta Crystallogr. Sect. A.* 32 (1976) 751–767.  
doi:10.1107/S0567739476001551.
- [25] C. Gupta, H. Singh, *Uranium Resource Processing: Secondary Resources*, 1st ed., Springer-Verlag Berlin Heidelberg, 2003.
- [26] A. Napoli, Complex formation of iron(III) with diglycolic and iminodiacetic acids, *J. Inorg. Nucl. Chem.* 34 (1972) 987–997. doi:10.1016/0022-1902(72)80076-9.
- [27] J. Jiang, J.C. Renshaw, M.J. Sarsfield, F.R. Livens, D. Collison, J.M. Charnock, H. Eccles, Solution chemistry of uranyl ion with iminodiacetate and oxydiacetate: A combined NMR/EXAFS and potentiometry/calorimetry study, *Inorg. Chem.* 42 (2003) 1233–1240.  
doi:10.1021/ic020460o.
- [28] A.E. Martell, R.M. Smith, R.J. Motekaitis, *NIST Database 46*, Natl. Inst. Stand. Technol. (2001).
- [29] J. Jiang, M.J. Sarsfield, J.C. Renshaw, F.R. Livens, D. Collison, J.M. Charnock, M. Helliwell, H. Eccles, Synthesis and Characterisation of Uranyl Compounds with Iminodiacetate and Oxydiacetate Displaying Variable Denticity, *Inorg. Chem.* 41 (2002) 2799–2806.
- [30] L. Downward, C.H. Booth, W.W. Lukens, F. Bridges, A variation of the F-test for determining statistical relevance of particular parameters in EXAFS fits, *AIP Conf. Proc.* 882 (2007) 129–131. doi:10.1063/1.2644450.
- [31] W.C. Hamilton, Significance Tests on the Crystallographic R Factor\*, *Acta Cryst.* 18 (1965) 502–510.
- [32] C. Hennig, K. Schmeide, V. Brendler, H. Moll, S. Tsushima, A.C. Scheinost, The Structure of Uranyl Sulfate in Aqueous Solution - Monodentate Versus Bidentate Coordination, in: 13th

Int. Proc. X-Ray Absorpt. Fine Struct., Stanford, 2006: pp. 262–264.

- [33] Y.-L. Wang, L. Zhu, B.-L. Guo, S.-W. Chen, W.-S. Wu, Mesoporous silica SBA-15 functionalized with phosphonate and amino groups for uranium uptake, *New J. Chem.* 38 (2014) 3853–3861. doi:10.1007/s11426-012-4625-7.
- [34] N. V. Jarvis, J.M. Wagener, Mechanistic studies of chelating resins using two-phase potentiometry, *Talanta.* 41 (1994) 747–754. doi:10.1016/0039-9140(93)E0040-K.
- [35] M.D. Ogden, E.M. Moon, A. Wilson, S.E. Pepper, Application of chelating weak base resin Dowex M4195 to the recovery of uranium from mixed sulfate/chloride media, *Chem. Eng. J.* 317 (2017) 80–89. doi:10.1016/j.cej.2017.02.041.